Development of the Yearly Mode-1 M_2 Internal Tide Model in 2019

Zhongxiang Zhao
Applied Physics Laboratory, University of Washington, Seattle, Washington

Zhao., Z, 2022: Development of the yearly mode-1 M_2 internal tide model in 2019. *J. Atmos. Oceanic Technol.*, 39, 463–478, https://doi.org/10.1175/JTECH-D-21-0116.1.

Introduction

This work is motivated to study the interannual variation of internal tides using observation-based yearly internal tide models from satellite altimetry. Previous satellite observations of internal tides are usually based on 25 years of altimeter data from 1993 to 2017. The yearly subsetted altimeter data are short, so that the resultant yearly models would be overwhelmed by noise. A new mapping technique is developed and demonstrated in this work. This work demonstrates that yearly internal tides can be observed by concurrent altimetry missions and their interannual variations can be determined. It paves a path to study the interannual and decadal variations of internal tides on a global scale and monitor the global ocean changes by tracking long-range internal tides.

The yearly mode-1 M_2 internal tide model in 2019 is constructed using sea surface height (SSH) measurements made by six concurrent satellite altimetry missions: Jason-3, Sentinel-3A, Sentinel-3B, CryoSat-2, Haiyang-2A, and SARAL/AltiKa. The model is developed following a three-step procedure consisting of two rounds of plane wave analysis with a spatial bandpass filter in between. Prior mesoscale correction is made on the altimeter data using AVISO gridded mesoscale fields. The model is labeled Y2019, because it represents the 1-yr-coherent internal tide field in 2019. In contrast, the model developed using altimeter data from 1992 to 2017 is labeled MY25, because it represents the multiyear-coherent internal tide field in 25 years.

Thanks to the new mapping technique, model errors in Y2019 are as low as those in MY25. Evaluation using independent altimeter data confirms that Y2019 reduces slightly less variance (~6%) thanMY25. Comparing Y2019 and MY25 shows that mode-1 M_2 internal tides are subject to significant interannual variability in both amplitude and phase, and their interannual variations are a function of location. This mapping technique has been applied successfully to 2017 and 2018.

Data

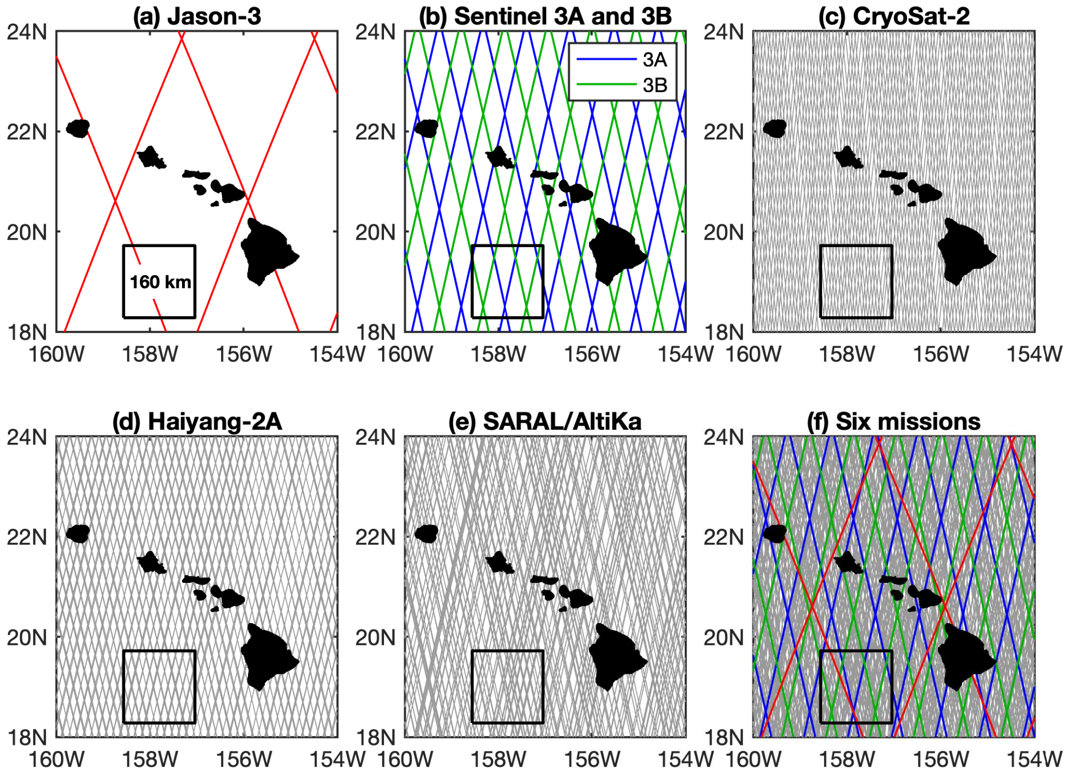

Ground tracks of six concurrent altimetry missions in 2019: (a) Jason-3, (b) Sentinel-3A and Sentinel-3B, (c) CryoSat-2, (d) Haiyang-2A, (e) SARAL/AltiKa, and (f) all six altimetry missions. Jason-3, Sentinel-3A, and Sentinel-3B are exact-repeat missions. CryoSat-2, Haiyang-2A, and SARAL/AltiKa are nonrepeat missions. All missions have SSH measurements in multiple years, but their data are trimmed to 2019 to construct yearly internal tide models. Black boxes indicate the 160 km x 160 km fitting window in this study.

The internal tide model Y2019 will be compared with the 25-yr-coherent model MY25 that is constructed using 25 years of satellite altimeter data from 1993 to 2017.

Mission	Orbit	Repeat period (days)	No. of tracks	Track interval (km)
Jason-3	Exact-repeat track	9.9156	254	315
Sentinel-3A	Exact-repeat track	27	770	100
Sentinel-3B	Exact-repeat track	27	770	100
CryoSat-2	Long-repeat track	369	10 688	7.5
Haiyang-2A	Geodetic track	168	4630	17.3
SARAL/AltiKa	Drifting track	35	1002	~80

Methods

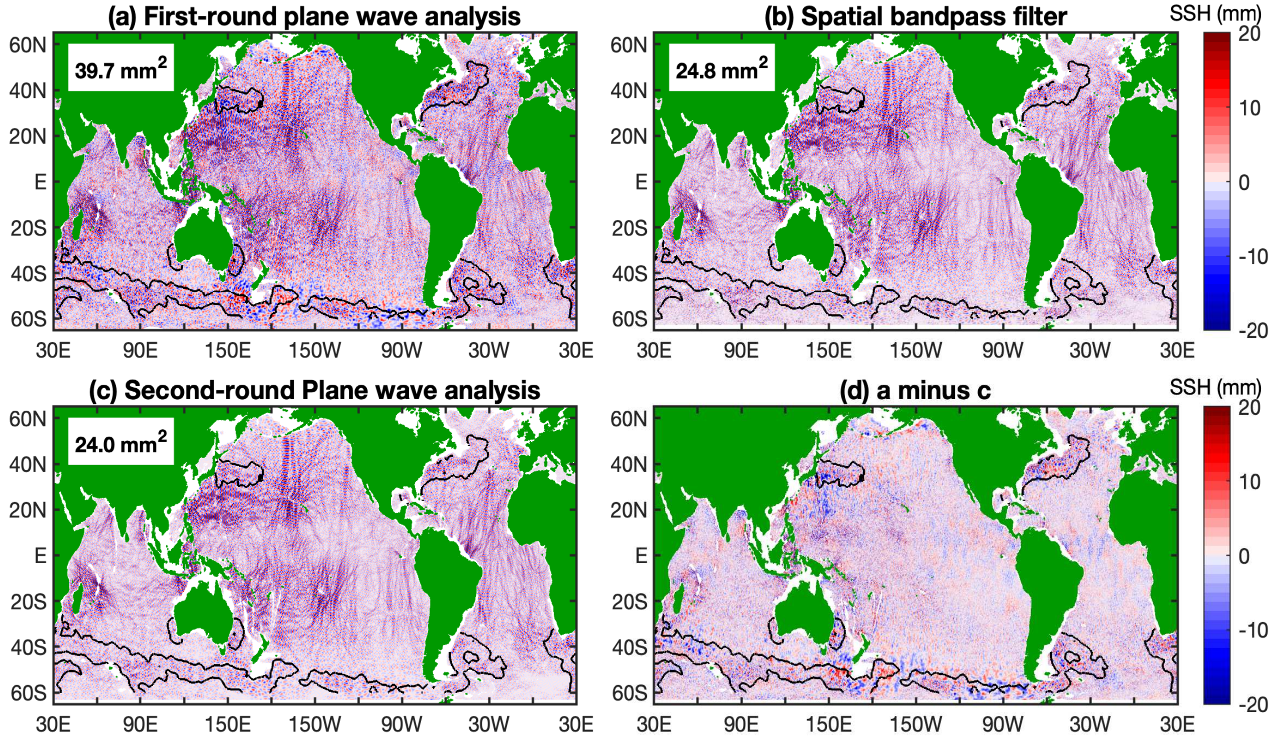

Mode-1 M_2 internal tides are extracted following a three-step mapping technique developed by the author. It consists of two rounds of plane wave analysis with a spatial bandpass filter in between (Table below). The example shows the intermediate internal tide fields obtained in each of the three steps in Y2019.

(left) Mode-1 M_2 internal tides are mapped using altimeter data in 2019. (a) Internal tides obtained by the first-round plane wave analysis. (b) Internal tides cleaned by spatial bandpass filtering. (c) Internal tides obtained by the second-round plane wave analysis. (d) The difference between (a) and (c). Black contours indicate regions of strong currents.

Model	Y2019 (Y2019test)	MY25
Time coverage	2019	1993–2017
Altimetry missions	*Jason-3*, *Sentinel-3A*, *Sentinel-3B*, *CryoSat-2*, *Haiyang-2A*, *SARAL*/AltiKa	TOPEX/Poseidon, *Jason-1*/-*2*/-*3*, *ERS-2*, *Envisat*, *Geosat Follow-On*
Data record	6 satellite years	54 satellite years
Preprocess	Mesoscale correction (along-track high-pass filter)	No filter
Step 1	Plane wave analysis: 0.2° lon × 0.2° lat, 160 km × 160 km, 5 waves	
Step 2	Spatial bandpass filter: 850 × 850 km, [0.8 1.25] × *K*(lon, lat)	
Step 3	Plane wave analysis: 0.2° lon × 0.2° lat; 160 km ×160 km; 5 waves	

M_2 internal tide models in 2019

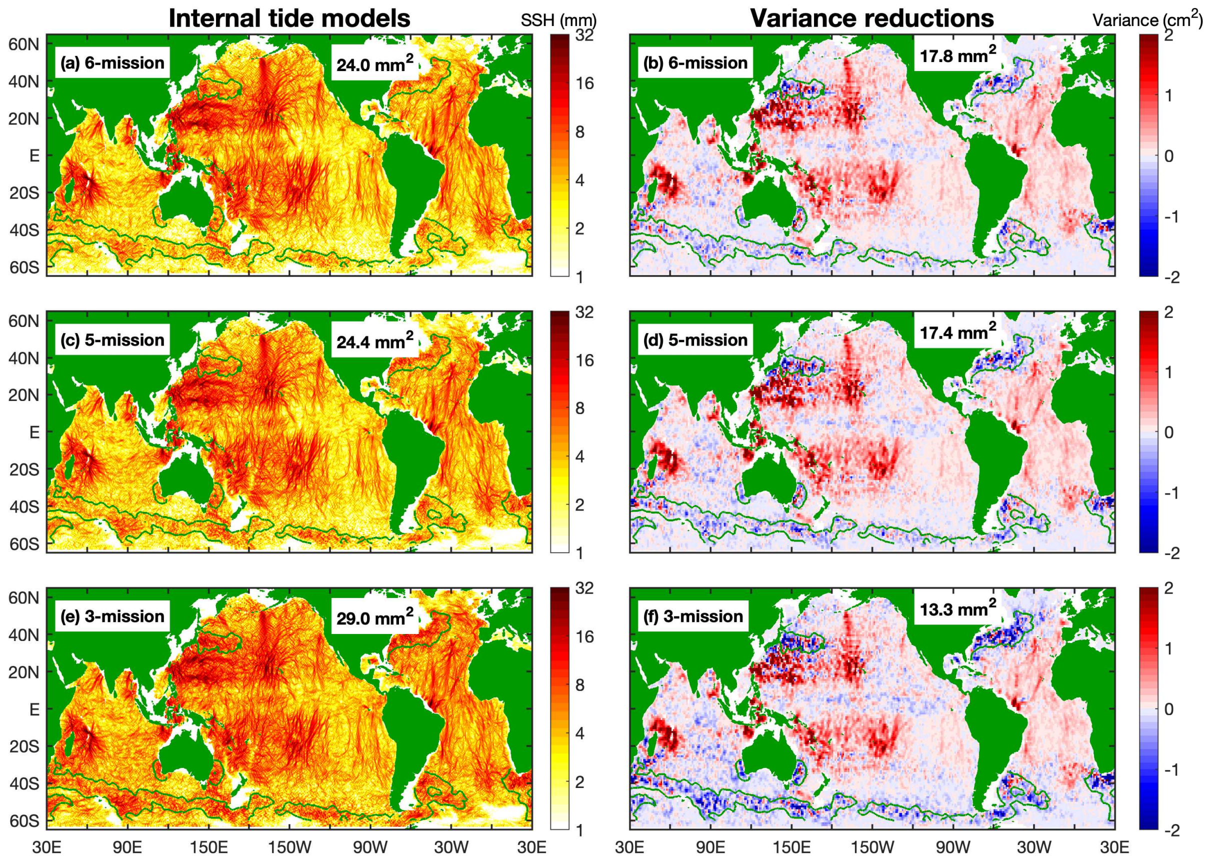

Internal tide models are constructed using fewer altimetry missions in 2019. The motivation question is whether mode-1 M_2 internal tide models can be constructed or not when there are fewer altimetry missions in one given year. Here three mode-1 M_2 internal tide models are mapped using altimeter data from fewer missions following the same mapping procedure.

The results suggest that Y2019-6m and Y2019-5m are of same quality. Mode-1 M_2 internal tide model can be constructed using five altimetry missions in one year. However, Y2019-3m has a relatively poor quality.

Internal tide models constructed using altimetry missions in 2019. (left) Internal tide models. (right) Variance reductions obtained in making internal tide correction to altimeter data in 2018. (a),(b) Six altimetry missions (Y2019-6m). (c),(d) Five altimetry missions (Y2019-5m). (e),(f) Three nonrepeat altimetry missions (Y2019-3m). Numbers are global mean model variances or variance reductions (excluding regions of strong currents).

Phase difference between Y2019 and MY25

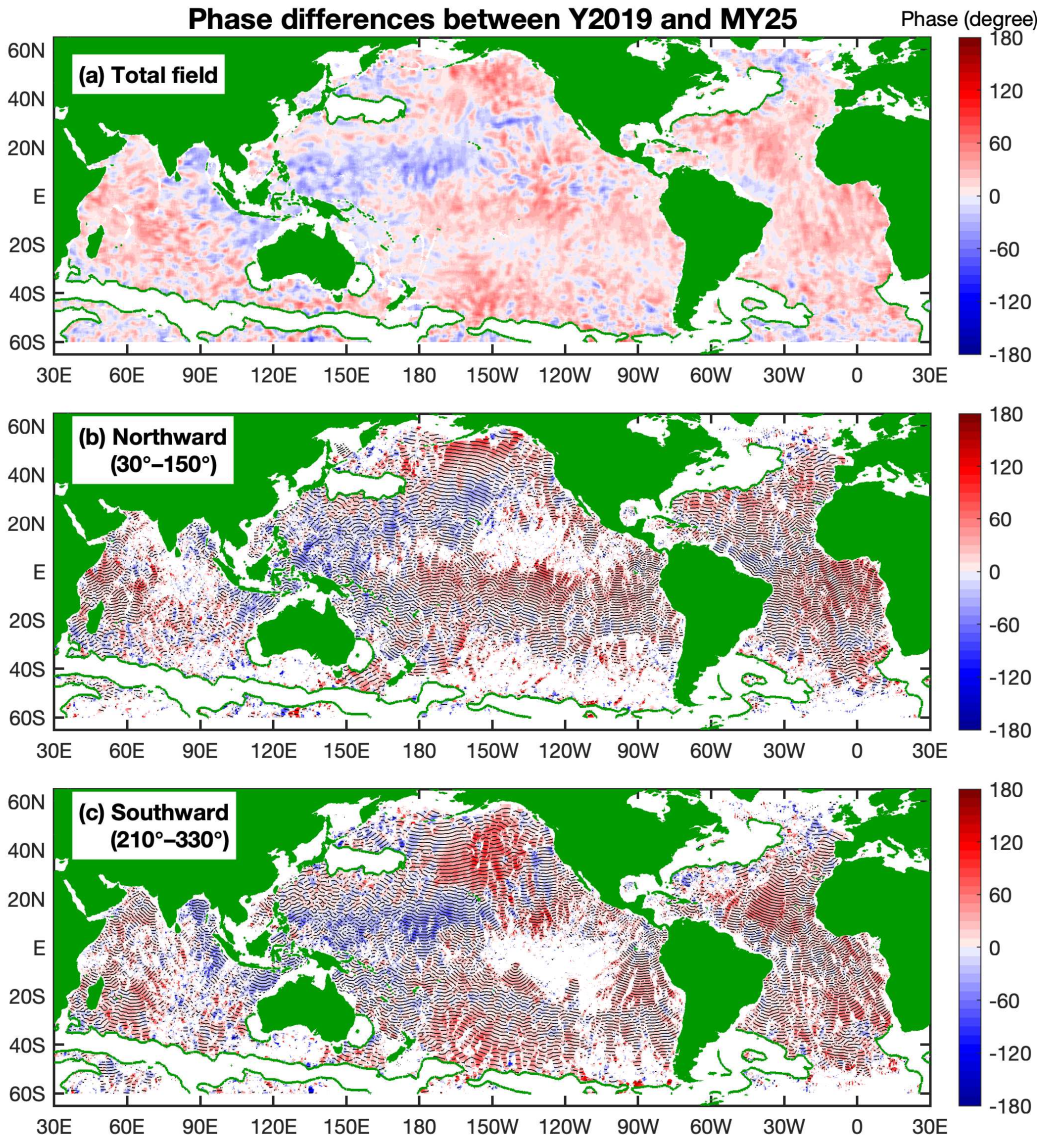

Phase differences between Y2019 and MY25. Positive and negative values mean that internal tides in Y2019 travel faster and slower, respectively. (a) Total field. (b) Northward component. (c) Southward component. Shown are pointwise differences smoothed by two-dimensional 11-point running mean. Green contours indicate regions of strong currents. In (b) and (c), internal tides with SSH amplitudes <1 mm or in regions of strong currents are not shown.

Negative phase differences in the western Pacific and eastern Indian Oceans, and positive phase differences in the eastern Pacific, western Indian, and Atlantic Oceans. For example, negative phase differences can be clearly seen in the Bay of Bengal and the Indonesian Seas. The southward internal tides from the Lombok Strait have negative phase differences, which means that internal tides have slower speeds in 2019. One important feature is the change (increase or decrease) of phase differences along long-range internal tidal beams.

Note that positive and negative phase differences mean internal tides travel faster and slower in Y2019, respectively. Information on ocean stratification can be inferred from phase differences.

Long-range mode-1 M_2 internal tidal beam

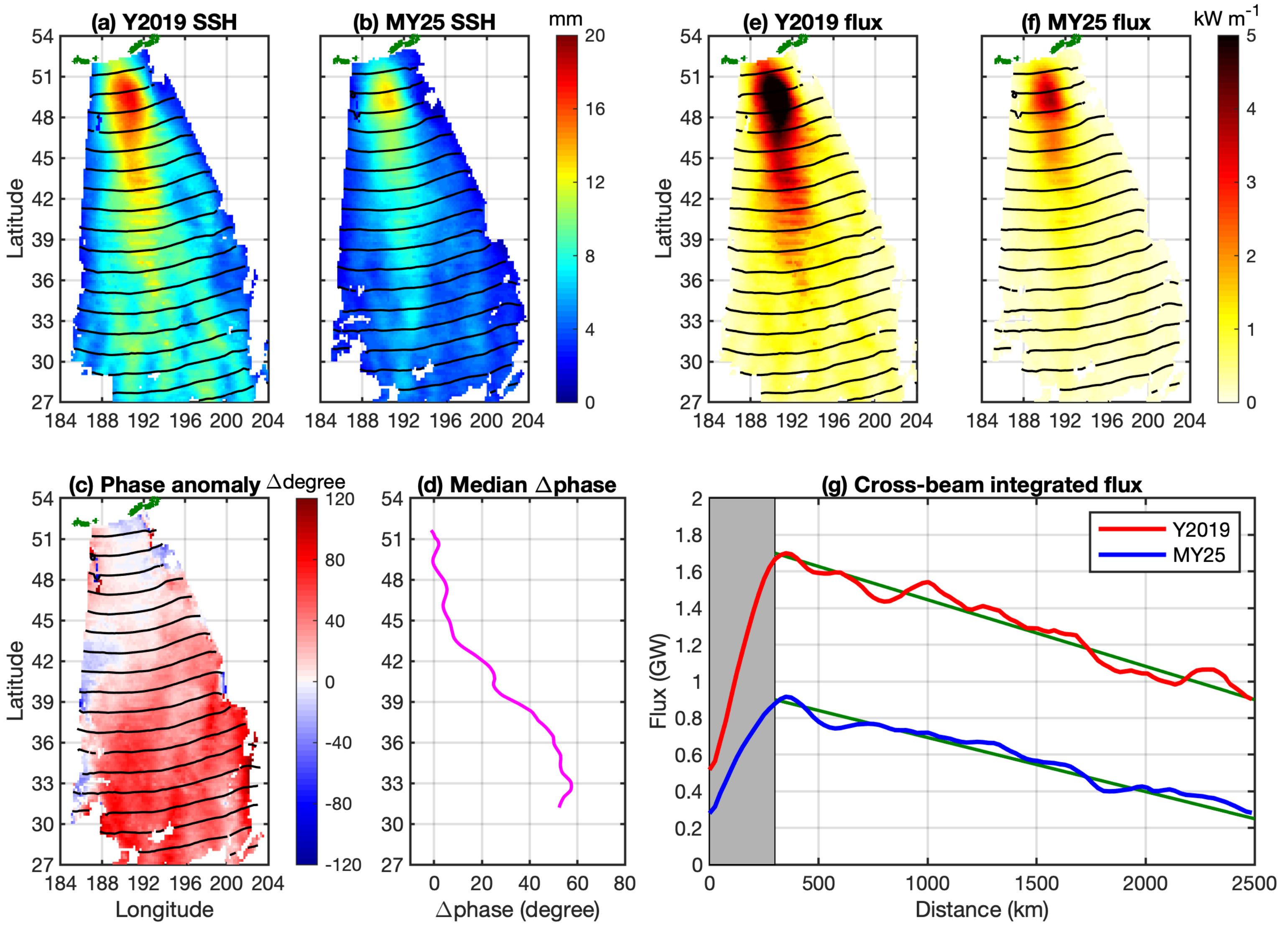

Long-range southward M_2 internal tides from Amukta Pass, Alaska. (a) Y2019 SSH amplitude. (b) MY25 SSH amplitude. (c) Phase anomaly of Y2019 with respect to MY25. Positive values mean that internal tides travel faster in Y2019. (d) Median phase anomaly as a function of latitude, showing that the phase anomaly increases from 0 in the near field to 60 degrees in the far field. Black lines are Greenwich co-phase charts. (e) Y2019 energy flux. (f)MY25 energy flux. (g) Cross beam integrated energy fluxes as a function of propagation distance. The energy flux in Y2019 is about twice that in MY25.

The total travel time is about 185 h (15 M_2 cycles). The percentage change along the beam is 1.1%, which is barely detectable by pointwise measurements. Fortunately, the weak signal is amplified with internal tide propagation. In the far field, it is amplified by 15 times, and can be unambiguously detected.

M_2 internal tide models in 2017, 2018, and 2019

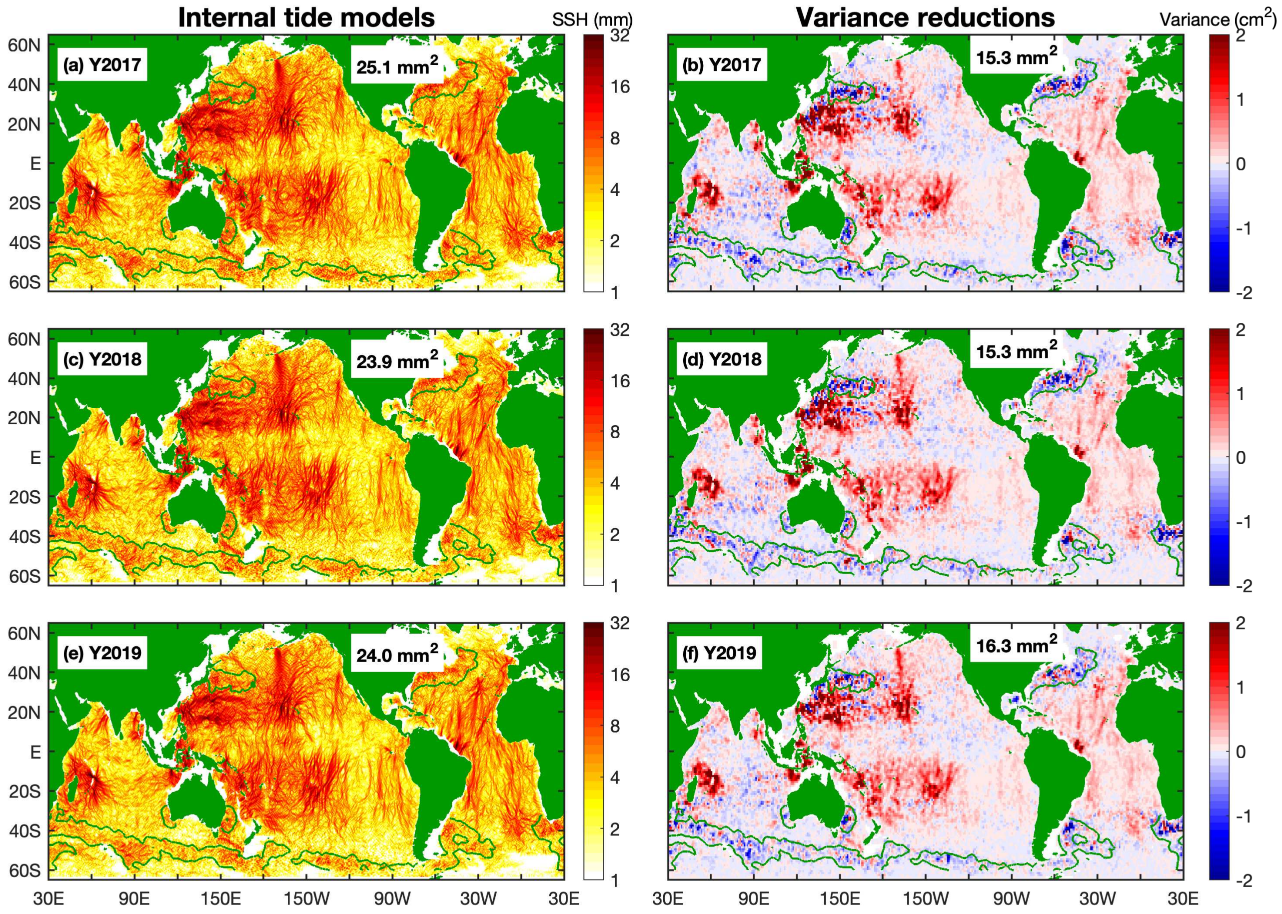

This new mapping technique has been applied successfully to other years. The work here discusses the internal tide models in 2017 and 2018. There are six concurrent altimetry missions in 2017 and five missions in 2018. All models are constructed following the same procedure and using the same parameters. The resultant three internal tide models have similar spatial patterns and close model variances. Evaluation using independent altimeter data in 2020 confirms that they have similar performances in making internal tide correction.

Internal tide models constructed using yearly altimeter data in 2017, 2018, and 2019. (left) Internal tide models. (right) Variance reductions obtained in making internal tide correction to altimeter data in 2020. Green contours indicate regions of strong currents. Numbers are global mean model variances or variance reductions (excluding regions of strong currents).

Phase anomalies in 2017 and 2018

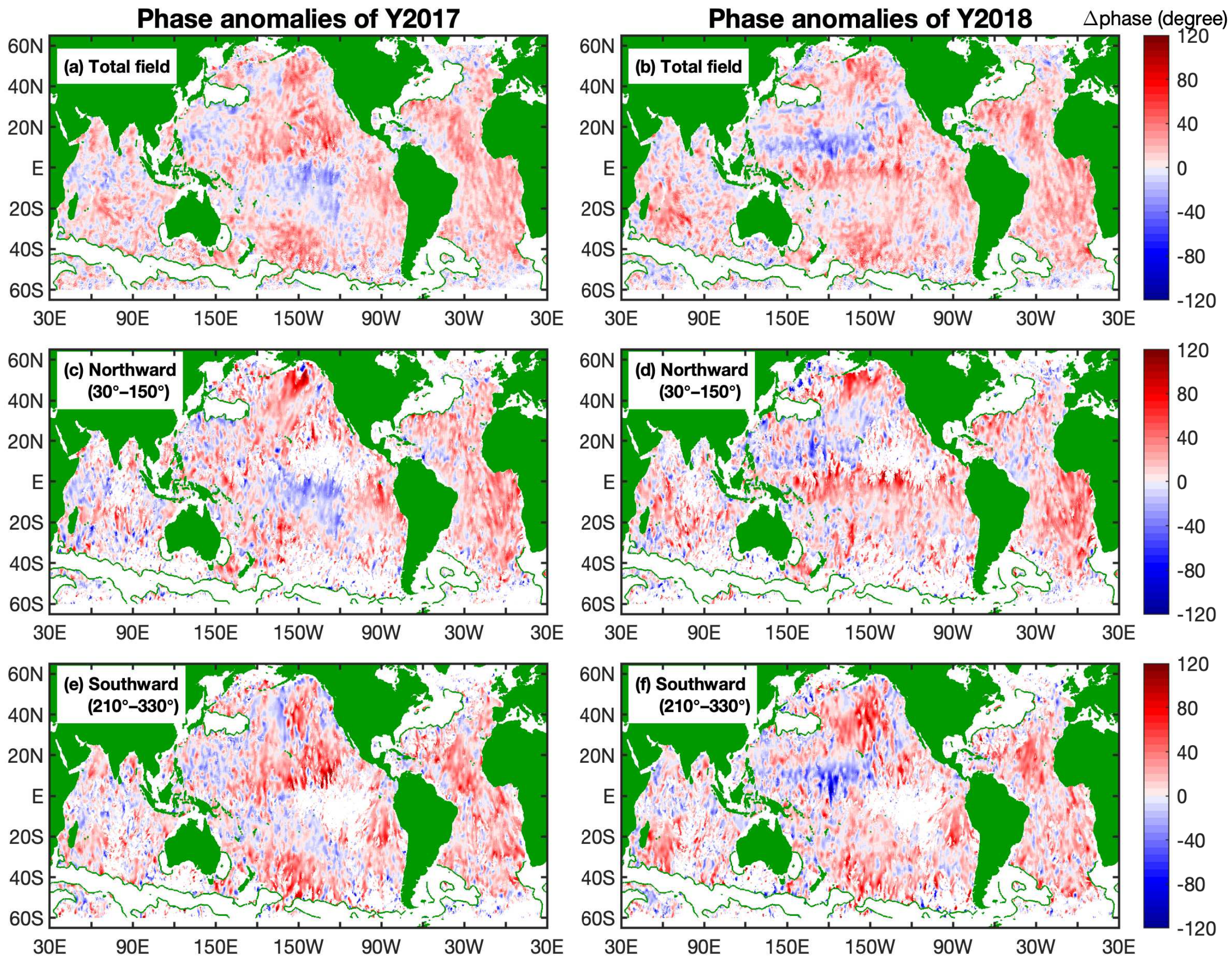

Phase anomalies of (a) Y2017 and (b) Y2018 with respect to MY25. (a),(b) The total field. (c),(d) The northward component. (e),(f) The southward component. Green contours indicate regions of strong currents. Internal tides with SSH amplitudes <1 mm or in regions of strong currents are not shown.

Both Y2017 and Y2018 show spatially coherent patterns, confirming that the phase anomalies are real signals, instead of model errors. These models have different phase anomalies, suggesting the interannual variations of internal tides. One remarkable feature is that, in 2017, one negative-value region is in the southern central Pacific Ocean. In 2018, this region moves to the northern central Pacific Ocean. Furthermore, this negative value region moves to the western Pacific Ocean in 2019. This feature is likely caused by large-scale ocean oscillations. Further examination of its driving mechanism is worthwhile.

Conclusions

It is challenging to construct robust internal tide models using yearly subsetted altimeter data. This paper addresses this challenge by developing a new mapping technique. There are six concurrent satellite altimetry missions, exact repeat or nonrepeat, in 2019. This paper shows that yearly mode-1 M_2 internal tide model in 2019 can be constructed using the six (even five) altimetry missions.

This work shows that mode-1 M_2 internal tides can be extracted from five or six concurrent altimetry missions in one given year. This achievement is attributed to some indispensable steps in the new mapping technique. Plane wave analysis suppresses model errors by using more independent data in one fitting window. The spatial bandpass filter is indispensable in suppressing model noise.

Comparing Y2019 and MY25 reveals that mode-1 M_2 internal tides are subject to significant interannual variability in both amplitude and phase. The interannual variations of internal tides are a function of location. The interannual variations of internal tides can be better studied using the decomposed internal tide components by propagation direction.

This mapping technique has been applied successfully to 2017 and 2018 The phase anomalies in 2017, 2018, and 2019 have different spatial patterns, suggesting the interannual variations of internal tides caused by large-scale ocean changes. It is expected that the interannual variations of internal tides can be quantified using yearly internal tide models from satellite altimetry.